

This is a repository copy of *Using Parahydrogen to Hyperpolarize Amines, Amides, Carboxylic Acids, Alcohols, Phosphates and Carbonates*.

White Rose Research Online URL for this paper:

<https://eprints.whiterose.ac.uk/id/eprint/125921/>

Version: Published Version

---

**Article:**

Iali, Wissam orcid.org/0000-0002-9428-2023, Rayner, Peter J. orcid.org/0000-0002-6577-4117 and Duckett, Simon B. orcid.org/0000-0002-9788-6615 (2018) Using Parahydrogen to Hyperpolarize Amines, Amides, Carboxylic Acids, Alcohols, Phosphates and Carbonates. *Science Advances*. eaao6250. ISSN 2375-2548

<https://doi.org/10.1126/sciadv.aao6250>

---

**Reuse**

This article is distributed under the terms of the Creative Commons Attribution (CC BY) licence. This licence allows you to distribute, remix, tweak, and build upon the work, even commercially, as long as you credit the authors for the original work. More information and the full terms of the licence here:

<https://creativecommons.org/licenses/>

**Takedown**

If you consider content in White Rose Research Online to be in breach of UK law, please notify us by emailing [eprints@whiterose.ac.uk](mailto:eprints@whiterose.ac.uk) including the URL of the record and the reason for the withdrawal request.

## CHEMICAL PHYSICS

Using *parahydrogen* to hyperpolarize amines, amides, carboxylic acids, alcohols, phosphates, and carbonates

Wissam Iali, Peter J. Rayner, Simon B. Duckett\*

Hyperpolarization turns weak nuclear magnetic resonance (NMR) and magnetic resonance imaging (MRI) responses into strong signals, so normally impractical measurements are possible. We use *parahydrogen* to rapidly hyperpolarize appropriate  $^1\text{H}$ ,  $^{13}\text{C}$ ,  $^{15}\text{N}$ , and  $^{31}\text{P}$  responses of analytes (such as  $\text{NH}_3$ ) and important amines (such as phenylethylamine), amides (such as acetamide, urea, and methacrylamide), alcohols spanning methanol through octanol and glucose, the sodium salts of carboxylic acids (such as acetic acid and pyruvic acid), sodium phosphate, disodium adenosine 5'-triphosphate, and sodium hydrogen carbonate. The associated signal gains are used to demonstrate that it is possible to collect informative single-shot NMR spectra of these analytes in seconds at the micromole level in a 9.4-T observation field. To achieve these wide-ranging signal gains, we first use the signal amplification by reversible exchange (SABRE) process to hyperpolarize an amine or ammonia and then use their exchangeable NH protons to relay polarization into the analyte without changing its identity. We found that the  $^1\text{H}$  signal gains reach as high as 650-fold per proton, whereas for  $^{13}\text{C}$ , the corresponding signal gains achieved in a  $^1\text{H}$ - $^{13}\text{C}$  refocused insensitive nuclei enhanced by polarization transfer (INEPT) experiment exceed 570-fold and those in a direct-detected  $^{13}\text{C}$  measurement exceed 400-fold. Thirty-one examples are described to demonstrate the applicability of this technique.

## INTRODUCTION

Nuclear magnetic resonance (NMR) is one of the most powerful methods for the study of materials, and magnetic resonance imaging (MRI) plays a vital role in clinical diagnosis. However, the low sensitivity of these techniques limits their applicability. The hyperpolarization method dynamic nuclear polarization (DNP) improves the detectability of analytes such as pyruvate to the level that the MRI-based diagnosis of disease is now possible (1). *Parahydrogen* ( $p\text{-H}_2$ ), which is cheap to prepare and exists as a pure nuclear spin state, was shown to enhance the strength of an NMR signal in 1987 (2), although these methods have not yet been used clinically. This may reflect the fact that  $p\text{-H}_2$  was originally used to sensitize chemically modified hydrogenation products (3, 4), and only recently has a method been developed where the original identity of the sensitized analyte is retained (5). This approach, signal amplification by reversible exchange (SABRE), harnesses  $p\text{-H}_2$  in the form of metal-bound hydride ligands and transfers hyperpolarization into a weakly bound substrate (6–8) via the small  $J$ -couplings that connect them (9). Ligand exchange then builds up a pool of hyperpolarized substrate according to Scheme 1A (10). SABRE is successful for analytes with multiple bonds to nitrogen such as nicotinamide (11), isoniazid (12), pyrazole (13), and acetonitrile (14), with  $^1\text{H}$  polarizations of 50% (11) and  $^{15}\text{N}$  values of 20% (15) being achieved. Furthermore, although it works for other nuclei (11, 16–20), it fails to sensitize many classes of analytes.

Here, we describe a method where  $p\text{-H}_2$  hyperpolarizes a range of amines, amides, carboxylic acids, alcohols, phosphates, and carbonates without changing their chemical identity. Our method starts with the hyperpolarization of ammonia (the hyperpolarization transfer agent). Subsequently, polarization is relayed into the specified analyte through proton exchange, as outlined in Scheme 1B. Spontaneous low-field transfer then creates the hyperpolarized analyte, which we detect. We called this approach SABRE-RELAY and predict that, when it is fully optimized, it will have a major impact on NMR and MRI in accordance with the fact that we exemplify it for 31 analytes.

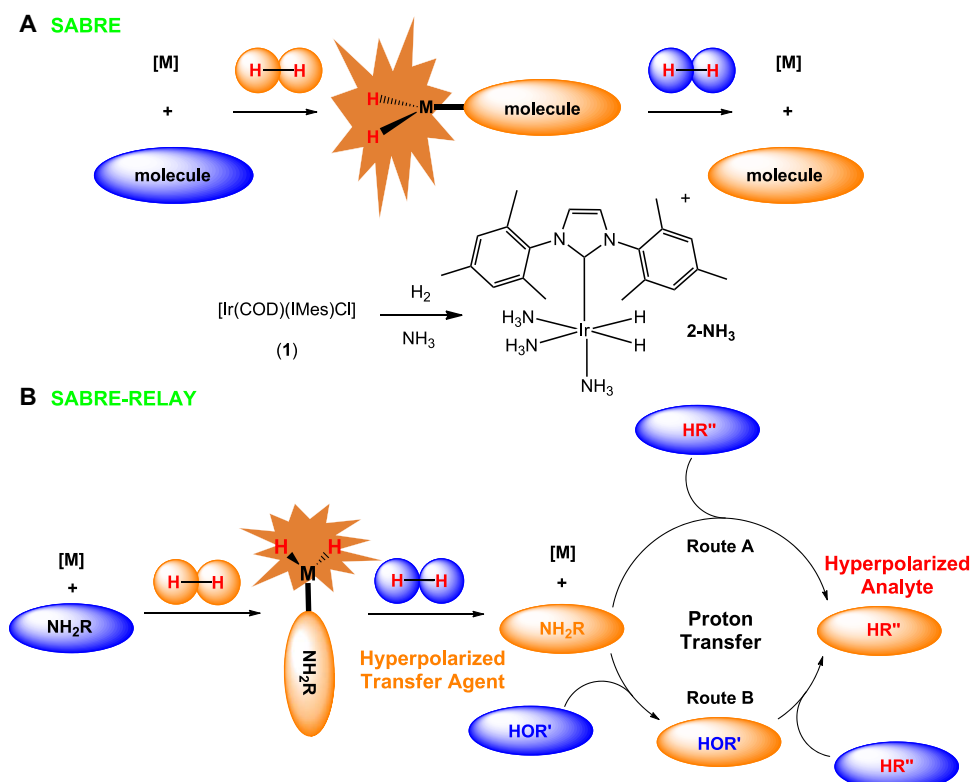
## RESULTS

We achieve SABRE-RELAY by reacting ammonia with the most versatile of the current SABRE catalysts,  $[\text{IrCl}(\text{COD})(\text{IMes})]$  (21, 22) (1) [where IMes is 1,3-bis(2,4,6-trimethylphenyl)imidazol-2-ylidene and COD is cycloocta-1,5-diene] and  $\text{H}_2$ , to form  $[\text{Ir}(\text{H})_2(\text{IMes})(\text{NH}_3)_3]\text{Cl}$  (2-NH<sub>3</sub>) according to Scheme 1. When this reaction is completed in dichloromethane- $d_2$ , 2-NH<sub>3</sub> exhibits equatorial and axial NH<sub>3</sub> ligand signals at  $\delta$  2.19 and 2.88 in the corresponding  $^1\text{H}$  NMR spectrum, alongside a broad NH<sub>3</sub> response at  $\delta$  0.47, as detailed in Fig. 1A. When this sample is examined after exposure to a 2-bar pressure of  $p\text{-H}_2$  gas at 60 G, the resulting  $^1\text{H}$  NMR signal for free NH<sub>3</sub> now shows an ~10-fold signal enhancement per proton, with the bound NH<sub>3</sub> ligand signal at  $\delta$  2.19 showing a 3-fold enhanced response. These observations confirm that 2-NH<sub>3</sub> undergoes SABRE to produce hyperpolarized ammonia. When the same process is repeated in methanol- $d_4$ , 2-NH<sub>3</sub> exhibits a hydride resonance at  $\delta$  -23.2 that rapidly separates into several components as H-D exchange proceeds to form an array of isotopologues. However, when  $p\text{-H}_2$  is used, a hyperpolarized NMR signal is readily seen at  $\delta$  5.06 for the exchangeable proton of  $\text{CD}_3\text{OH}$ , which exhibits a 32-fold intensity gain over its thermally equilibrated signal. Therefore, we added a 5% loading of  $\text{H}_2\text{O}$ , relative to iridium, to the  $\text{CD}_2\text{Cl}_2$  sample and reexamined it. Under these conditions, the free NH<sub>3</sub> signal gain resulting from SABRE proved to increase to 40-fold per proton, whereas the corresponding equatorial ligand signal now showed an 85-fold per proton gain (Fig. 1B). In addition, the free  $\text{H}_2\text{O}$  signal was enhanced by 75-fold per proton, a result that compares well with other solvent signal enhancements (23–25).

Exchange spectroscopy measurements were then used to confirm that free NH<sub>3</sub> and the equatorially bound NH<sub>3</sub> ligand of 2-NH<sub>3</sub> are in chemical exchange, with the observation of further exchange peaks between free NH<sub>3</sub> and  $\text{H}_2\text{O}$  demonstrating the rapid transfer of protons between them. On the basis of this selectivity, we conclude that, when the ammonia is bound, proton exchange between NH<sub>3</sub> and  $\text{H}_2\text{O}$  is suppressed because the nitrogen lone pair is involved in bonding to the metal center. Consequently, it now becomes hyperpolarized by SABRE. Proton exchange proceeds, though, after NH<sub>3</sub> dissociation, and this leads to the observation of hyperpolarization in the chemical exchange-averaged

Copyright © 2018  
The Authors, some  
rights reserved;  
exclusive licensee  
American Association  
for the Advancement  
of Science. No claim to  
original U.S. Government  
Works. Distributed  
under a Creative  
Commons Attribution  
License 4.0 (CC BY).

Department of Chemistry, University of York, Heslington, York YO10 5DD, UK.  
\*Corresponding author. Email: sbd3@york.ac.uk



**Scheme 1. (A) Hyperpolarization via SABRE and (B) hyperpolarization via SABRE-RELAY.** SABRE is used to hyperpolarize the transfer agent  $\text{NH}_2\text{R}$ , where R is H or  $\text{CH}_2\text{Ph}$  or  $\text{CH}_2\text{CH}_2\text{Ph}$  (etc.), which relays polarization to the analyte ( $\text{HR}''$ , route A), and  $\text{R}''$  is amide, carboxyl, phosphate, or alkoxide (etc.). This process involves both proton exchange and spin-spin interactions and may be mediated by an intermediary  $\text{HOR}'$ , where  $\text{R}'$  is H or suitable scaffold (route B). Center: Reaction scheme shows the formation of SABRE active **2-NH<sub>3</sub>**, which leads to  $\text{NH}_3$ .

response of  $\text{H}_2\text{O}$  (or  $\text{HOCD}_3$ ) according to Scheme 1B. Now, we show how it is possible to harness this proton exchange process to hyperpolarize the NMR signals of a series of added analytes.

First, we consider whether the SABRE hyperpolarization of  $\text{NH}_3$  can be relayed into the  $^1\text{H}$  and  $^{13}\text{C}$  responses of a series of alcohols  $\text{CH}_3(\text{CH}_2)_n\text{OH}$  (where  $n = 0$  to 7). To do this, we prepared a range of dichloromethane- $d_2$  solutions that contained  $[\text{Ir}(\text{H})_2(\text{IMes})(\text{NH}_3)_3]\text{Cl}$  (**2-NH<sub>3</sub>**),  $\text{NH}_3$ , and 1  $\mu\text{l}$  of each alcohol (typical concentration, 20 mM). After hyperpolarization transfer from  $p\text{-H}_2$ , strong signals resulted in the associated single-scan  $^1\text{H}$  NMR spectra, which reached up to 650-fold intensity gains per alcohol CH proton for 1-propanol, averaging at 265 across the series (see the Supplementary Materials). When the same  $p\text{-H}_2$  transfer process was undertaken and a fully coupled  $^{13}\text{C}$  NMR measurement was made instead of a  $^1\text{H}$  NMR measurement, molecule-diagnostic  $^{13}\text{C}$  and  $^1\text{H}$ - $^{13}\text{C}$  refocused insensitive nuclei enhanced by polarization transfer (INEPT)-based responses could also be recorded in one scan at 9.4 T for all the alcohols, as illustrated in Fig. 2B for 1-pentanol, with the associated signal gains reaching 570-fold for the  $\text{C}_\alpha$  signal of 1-hexanol. The SABRE-RELAY effect results in the detection of hyperpolarized NMR signals for all the spin-1/2 nuclei in these molecules. In addition, as with SABRE, the hyperpolarized NMR terms reflect a mixture of longitudinal single-spin and higher-order states, whose relative amplitudes depend on the magnetic field that the sample experiences during the polarization transfer step (16, 26). Furthermore, by reducing the concentrations of these analytes below the concentration of  $\text{NH}_3$ , it is possible to improve on SABRE-RELAY efficiency. This is beneficial when studying low-concentration analytes because

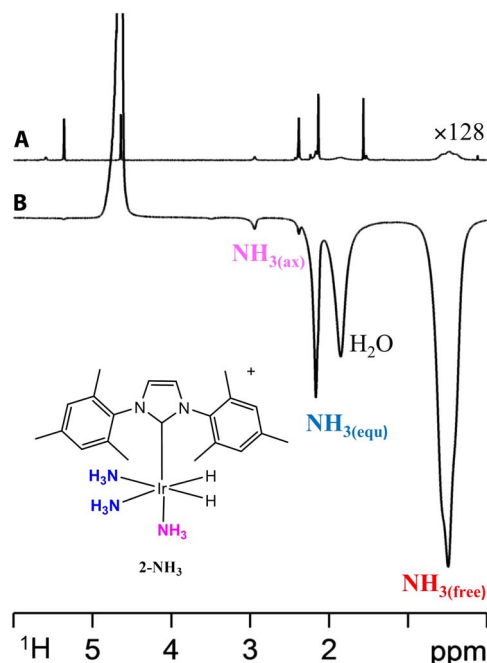


**Fig. 1. Hyperpolarization of  $\text{NH}_3$  under SABRE.** (A) Thermally polarized control  $^1\text{H}$  NMR spectrum showing peaks for **2-NH<sub>3</sub>**,  $\text{NH}_3$ , and  $\text{H}_2$  at 298 K in dichloromethane- $d_2$ ,  $\times 128$  vertical expansion relative to (B). (B) Corresponding single-scan  $^1\text{H}$  NMR spectrum in the presence of  $p\text{-H}_2$ , with the hyperpolarized responses for  $\text{H}_2\text{O}$ ,  $\text{NH}_{3(\text{free})}$ ,  $\text{Ir-NH}_{3(\text{equatorial})}$ , and  $\text{Ir-NH}_{3(\text{axial})}$  of **2-NH<sub>3</sub>** indicated.

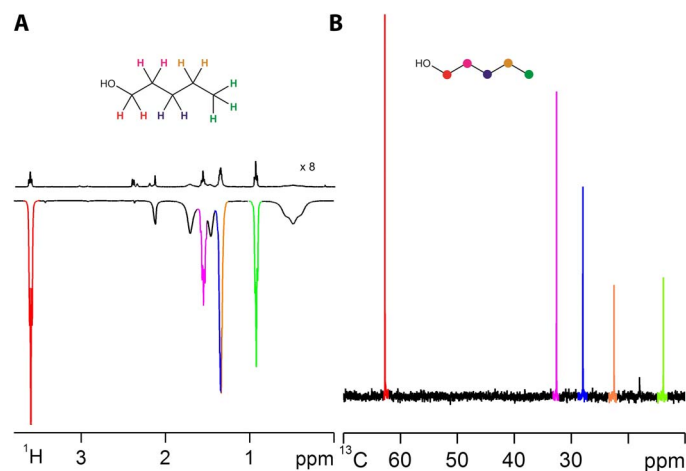


**Fig. 2.** Single-scan NMR spectra of 15.3 mM pentanol ( $\text{CH}_3\text{CH}_2\text{CH}_2\text{CH}_2\text{CH}_2\text{OH}$ , color-coded structure shown) in dichloromethane- $d_2$  solution resulting from the action of  $\text{NH}_3$ ,  $2\text{-NH}_3$ , and  $p\text{-H}_2$ . (A) Upper  $^1\text{H}$  NMR spectrum in the thermally polarized control,  $\times 8$  vertical expansion, relative to lower SABRE-RELAY spectrum. (B) Single-scan SABRE-RELAY  $^1\text{H}$ - $^{13}\text{C}$  refocused INEPT NMR spectrum (see fig. S8B for the corresponding thermal control trace).

when propanol was studied, the  $^1\text{H}$  NMR signal gains seen for its OH resonance increased by 100% on moving from a 15 to 1.5 mM concentration (fig. S4), whereas its CH resonances showed a ca. 50% improvement in enhancement level; a  $^1\text{H}$ - $^{13}\text{C}$  refocused INEPT response was still clearly visible in one scan, where the three signals from the OH end were 639, 538, and 603 times larger, respectively, than those in the corresponding  $^{13}\text{C}$  response. This polarization transfer method is also applicable to complex branched alcohols, and when a sample of  $^{13}\text{C}$ -labeled glucose was analyzed, a single-scan  $^{13}\text{C}$  response could be seen for all the expected  $\alpha$  and  $\beta$  form signals, which serves to illustrate the wider significance of this effect (fig. S15E). Furthermore, our studies show that, when SABRE-RELAY is carried out under anhydrous conditions with straight-chain alcohols, superior results are obtained.

Our next goal was to expand on the range of materials that can be sensitized by this method. We started with pyruvic acid but found that its addition to a solution of  $2\text{-NH}_3$  and  $\text{NH}_3$  resulted in ammonium salt precipitation, which acted to limit hyperpolarization efficacy. This can be overcome by the addition of a pH modifier such as  $\text{Cs}_2\text{CO}_3$ , but working with the corresponding sodium salt proved optimal. When  $^{13}\text{C}$ -labeled sodium pyruvate, acetate, or propanoic acid samples were studied in the presence of  $p\text{-H}_2$ , strong  $^1\text{H}$  and  $^{13}\text{C}$  signals were seen; the  $^{13}\text{C}$  signal gain for propionic acid was 109-fold. Furthermore, sodium dihydrogen phosphate, adenosine 5'-triphosphate disodium, and  $^{13}\text{C}$ -labeled sodium hydrogen carbonate provided strong  $^{31}\text{P}$  and  $^{13}\text{C}$  responses (Fig. 3, A and B), whereas the amides acetamide, urea, and methacrylamide showed substantial  $^1\text{H}$ ,  $^{13}\text{C}$ , and  $^{15}\text{N}$  signal gains; for urea, a  $^{13}\text{C}$  signal gain of 408-fold was observed. These studies could be completed with  $\text{NH}_3/\text{H}_2\text{O}$  or  $\text{NH}_3/\text{CH}_3\text{OH}$ , as detailed in the Supplementary Materials, to promote the necessary proton exchange, and the observations establish that analytes containing the four common functional groups—OH,  $\text{NH}_2\text{CO}$ , POH, and COOH—can be used. In some cases, we see evidence for Schiff-base condensation at long reaction times but could suppress this process by adding water.

To examine the role of the hyperpolarization transfer agent, we replaced  $\text{NH}_3$  with benzylamine ( $\text{BnNH}_2$ ) or phenethylamine (PEA).

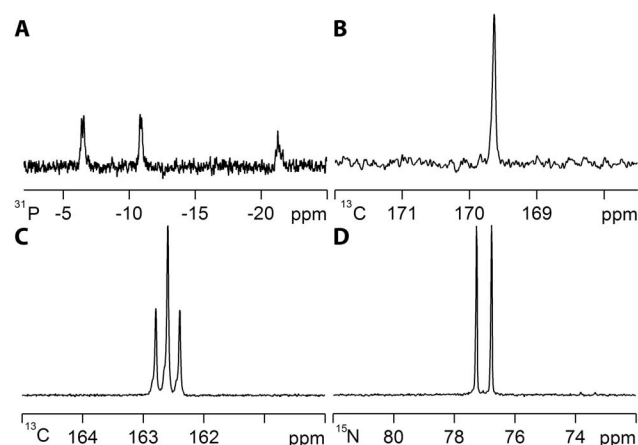


**Fig. 3.** Single-scan SABRE-RELAY NMR spectra recorded in dichloromethane- $d_2$  with  $\text{NH}_3$  and  $2\text{-NH}_3$  in the presence of  $p\text{-H}_2$ . (A) Sodium adenosine 5'-triphosphate,  $^1\text{H}$ - $^{31}\text{P}$  refocused INEPT spectrum (OH transfer) and (B) sodium  $^{13}\text{C}$ -labeled pyruvate,  $^{13}\text{C}$  NMR spectrum. Single-scan SABRE-RELAY NMR spectra recorded with PEA and  $2\text{-PEA}$  in the presence of  $p\text{-H}_2$  for (C)  $^{15}\text{N}$ - $^{13}\text{C}$ -labeled urea,  $^{13}\text{C}$  NMR spectrum, 25 mM concentration, and (D)  $^{15}\text{N}$ - $^{13}\text{C}$ -labeled urea,  $^{15}\text{N}$  NMR spectrum, 25 mM concentration. The corresponding thermally polarized spectra are detailed in figs. S29A, S18A, S23A, and S23C and yield no signal.

Both react with **1** and  $\text{H}_2$ , forming  $[\text{Ir}(\text{H})_2(\text{IMes})(\text{NH}_2\text{Bn})_3]\text{Cl}$  (**2-BnNH<sub>2</sub>**) and  $[\text{Ir}(\text{H})_2(\text{IMes})(\text{PEA})_3]\text{Cl}$  (**2-PEA**), respectively. For the corresponding **2-BnNH<sub>2</sub>** sample, signal gains for free  $\text{BnNH}_2$  of 72-fold (NH), 53-fold (CH), and 170-fold (aromatic), respectively, per proton are observed (Fig. 4), and these measurements can be repeated if the same sample is probed with  $p\text{-H}_2$  several days after the first observation was made. PEA proved to perform better than  $\text{BnNH}_2$ , with the corresponding  $\text{NH}_2$  signal gain being 108-fold per proton for a 10-fold loading of **1** with signal gains of 50-fold ( $\text{NCH}_2$ ), 45-fold ( $\text{CH}_2$ ), 92-fold (*ortho*), 50-fold (*meta*), and 20-fold (*para*) resulting for the other groups. These observations show how polarization transfer through the aliphatic carbon chain into the aromatic protons is possible.  $\text{BnNH}_2$  and PEA also proved suitable for SABRE-RELAY. In the case of PEA, the efficiency of urea hyperpolarization was found to improve (Fig. 3, C and D) over that achieved with  $\text{NH}_3$ , although the measured response of  $^{13}\text{C}$ -labeled glucose was found to reduce. Furthermore, replacing  $\text{BnNH}_2$  with its *dl*-form,  $\text{C}_6\text{D}_5\text{CD}_2\text{NH}_2$ , led to further improvements in observed analyte response level because the initially created SABRE hyperpolarization was now optimally focused into just the  $\text{NH}_2$  protons.

Given the wide range of amine  $\text{pK}_\text{b}$  values (27), it may be possible to remove the need for an auxiliary base when dealing with acidic analytes through a process of amine variation. Therefore, we conclude that studies on the role of the amine will be important for the optimization of SABRE-RELAY and may even allow the introduction of selectivity into the hyperpolarization process. Furthermore, because improvements in analyte detectability with SABRE can be easily achieved by varying the polarization transfer field, reducing relaxation within the analyte, and optimizing the catalyst lifetime while minimizing its relaxivity, we expect the signal gains reported here to be similarly improved upon in the future (5).

## DISCUSSION

In summary, we have shown that SABRE-RELAY can be used to hyperpolarize a wide range of biologically relevant materials. In the initial



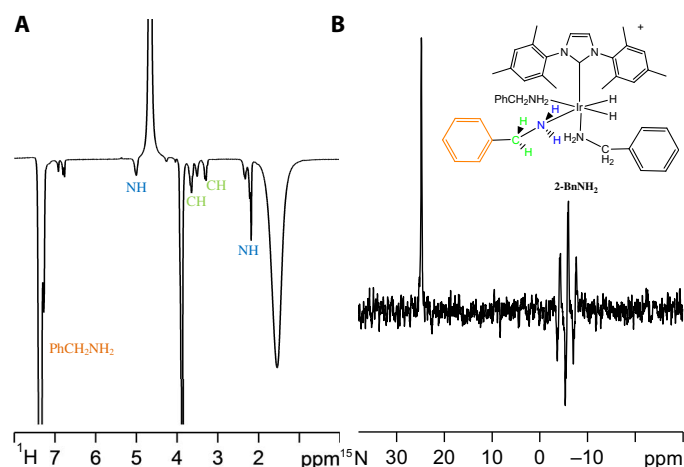


**Fig. 4. Hyperpolarization of benzylamine (BnNH<sub>2</sub>) under SABRE.** (A) <sup>1</sup>H NMR spectrum of hyperpolarized BnNH<sub>2</sub> achieved via **2-BnNH<sub>2</sub>** (top right) under SABRE in dichloromethane-*d*<sub>2</sub> solution after transfer at 60 G (see fig. S32A for the corresponding thermally equilibrated NMR spectrum). The enhanced signals are color-coded; NH<sub>2</sub> (blue), CH<sub>2</sub> (light green), and Ph (orange) for the bound equatorial BnNH<sub>2</sub> ligand of **2-BnNH<sub>2</sub>**. NH<sub>2</sub> and CH<sub>2</sub> of the free material, and H<sub>2</sub>O. (B) Corresponding <sup>15</sup>N NMR spectrum recorded using <sup>15</sup>N-labeled BnNH<sub>2</sub> after transfer in a μ-metal shield showing the free (left) and equatorial ligand (right) responses.

step, SABRE is used to enhance the NH proton response of the selected hyperpolarized transfer agent (the free amine) by between 10- and 120-fold per proton. When this is achieved in the presence of propanol, proton exchange results in its OH signal being amplified by between 250- and 500-fold. The nonequilibrium magnetic state of the OH proton is then successfully relayed into its aliphatic <sup>1</sup>H resonances such that the corresponding signals are amplified by between 650- and 790-fold per proton. We used this <sup>1</sup>H signal gain to record a single-scan <sup>1</sup>H-<sup>13</sup>C refocused INEPT NMR spectrum using just  $1 \times 10^{-7}$  moles of material, although direct transfer to <sup>13</sup>C means that a weaker fully coupled <sup>13</sup>C response can also be seen. On the basis of these signal gains, we hope that this route can be developed to allow the phenotyping of urine via lower-field <sup>13</sup>C detection in the future as an alternative to the current high-field <sup>1</sup>H detection methods (28). However, because exchangeable protons feature heavily in biochemical NMR, we expect harnessing this effect to be of significant interest to biochemists, especially if it is augmented with high-field transfer via the “low-irradiation generation of high tesla-SABRE” approach (29). In addition, because hyperpolarized urea, glucose, and pyruvate reflect successful MRI probes of disease (30, 31), when SABRE-RELAY is coupled with catalyst removal and biocompatibility, we expect this route to become clinically important because it can theoretically deliver a continuously hyperpolarized bolus (32). Moreover, because studies of catalysis with *p*-H<sub>2</sub> have made significant contributions to process optimization (33–37), we expect this approach to provide insight into important reactions such as transfer hydrogenation (38), hydroamination (39), and N<sub>2</sub> fixation in the future (40).

## MATERIALS AND METHODS

### Experimental design

The measurements undertaken in this work were completed on a 400-MHz Avance III spectrometer and involved <sup>1</sup>H, <sup>13</sup>C, <sup>15</sup>N, and <sup>31</sup>P detection, as detailed in the Supplementary Materials. Enhancement values were determined according to the methods defined here,

and sample details allowed the repetition of these measurements, which involved the following procedures.

### SABRE-RELAY polarization transfer method with NH<sub>3</sub>

The polarization transfer experiments that were reported in this study were conducted in 5-mm NMR tubes that were equipped with a J. Young's tap. Samples for these polarization transfer experiments were based on a 5 mM solution of [IrCl(COD)(IMes)] and the indicated substrate and NH<sub>3</sub> loadings in methanol-*d*<sub>4</sub> or dichloromethane-*d*<sub>2</sub> (0.6 ml). The samples were degassed before the introduction of NH<sub>3</sub>. Subsequently, *p*-H<sub>2</sub> at a pressure of ca. 3 bar was added. Then, samples were shaken for 10 s in the specified fringe field of an NMR spectrometer before they were rapidly transported into the magnet for subsequent interrogation by NMR spectroscopy. This whole process takes ca. 15 s to achieve.

### SABRE-RELAY polarization transfer method with BnNH<sub>2</sub> or PEA

The polarization transfer experiments that were reported were conducted in 5-mm NMR tubes that were equipped with a J. Young's tap. Samples for these polarization transfer experiments were based on a 5 mM solution of [IrCl(COD)(IMes)], the indicated BnNH<sub>2</sub> or PEA loading, and the indicated additional substrate at the specified loading in dichloromethane-*d*<sub>2</sub> (0.6 ml). The samples were degassed before the introduction of *p*-H<sub>2</sub> at a pressure of ca. 3 bar. Samples were then shaken for 10 s in the specified fringe field of an NMR spectrometer before they were rapidly transported into the magnet for subsequent interrogation by NMR spectroscopy.

## SUPPLEMENTARY MATERIALS

Supplementary material for this article is available at <http://advances.sciencemag.org/cgi/content/full/4/1/eaao6250/DC1>

- section S1. SABRE-RELAY polarization transfer method with NH<sub>3</sub>
- section S2. SABRE-RELAY polarization transfer method with BnNH<sub>2</sub> or PEA
- section S3. Polarization enhancement quantification procedures
- section S4. NMR spectrometer details
- section S5. Pulse sequence details
- section S6. SABRE-RELAY spectra
- fig. S1. INEPT pulse sequence.
- fig. S2. DEPT pulse sequence.
- fig. S3. SABRE-RELAY NMR spectra methanol.
- fig. S4. SABRE-RELAY NMR spectra ethanol.
- fig. S5. SABRE-RELAY NMR spectra propanol.
- fig. S6. SABRE-RELAY NMR spectra propanol, low concentration.
- fig. S7. SABRE-RELAY NMR spectra butanol.
- fig. S8. SABRE-RELAY NMR spectra pentanol.
- fig. S9. SABRE-RELAY NMR spectra hexanol.
- fig. S10. SABRE-RELAY NMR spectra heptanol.
- fig. S11. SABRE-RELAY NMR spectra octanol.
- fig. S12. SABRE-RELAY NMR spectra isopropanol.
- fig. S13. SABRE-RELAY NMR spectra *tert*-butanol.
- fig. S14. SABRE-RELAY NMR spectra *D*-glucose.
- fig. S15. SABRE-RELAY NMR spectra *D*-glucose-<sup>13</sup>C.
- fig. S16. SABRE-RELAY NMR spectra glycerol.
- fig. S17. SABRE-RELAY NMR spectra sodium acetate-<sup>13</sup>C.
- fig. S18. SABRE-RELAY NMR spectra sodium pyruvate-<sup>13</sup>C.
- fig. S19. SABRE-RELAY NMR spectra sodium acetate-1,2 <sup>13</sup>C<sub>2</sub>.
- fig. S20. SABRE-RELAY NMR spectra propionic acid-<sup>13</sup>C.
- fig. S21. SABRE-RELAY NMR spectra sodium hydrogen carbonate-<sup>13</sup>C.
- fig. S22. SABRE-RELAY NMR spectra urea-<sup>13</sup>C.
- fig. S23. SABRE-RELAY NMR spectra urea-<sup>13</sup>C-<sup>15</sup>N<sub>2</sub>.
- fig. S24. SABRE-RELAY NMR spectra urea-<sup>13</sup>C-<sup>15</sup>N<sub>2</sub>.
- fig. S25. SABRE-RELAY NMR spectra acetamide.
- fig. S26. SABRE-RELAY NMR spectra methacrylamide.
- fig. S27. SABRE-RELAY NMR spectra cyclohexyl methacrylamide.
- fig. S28. SABRE-RELAY NMR spectra mono sodium dihydrogen orthophosphate.

fig. S29. SABRE-RELAY NMR spectra adenosine 5'-triphosphate disodium salt.  
fig. S30. SABRE-RELAY NMR spectra ammonia in methanol.  
fig. S31. SABRE-RELAY NMR spectra ammonia in dichloromethane.  
fig. S32. SABRE-RELAY NMR spectra benzylamine.  
fig. S33. SABRE-RELAY NMR spectra benzylamine- $^{15}\text{N}$ .  
fig. S34. SABRE-RELAY NMR spectra, mixture of urea, propanol, and PEA.  
table S1. Alcohol  $^1\text{H}$  SABRE-RELAY signal enhancement values.  
table S2. Alcohol  $^{13}\text{C}$  SABRE-RELAY signal enhancement values.  
table S3. NMR data for **2-NH<sub>3</sub>**.  
table S4. NMR data for **2-BnNH<sub>2</sub>**.

## REFERENCES AND NOTES

- J. H. Ardenkjaer-Larsen, On the present and future of dissolution-DNP. *J. Magn. Reson.* **264**, 3–12 (2016).
- C. R. Bowers, D. P. Weitekamp, Parahydrogen and synthesis allow dramatically enhanced nuclear alignment. *J. Am. Chem. Soc.* **109**, 5541–5542 (1987).
- J. Natterer, J. Bargon, Parahydrogen induced polarization. *Prog. Nucl. Magn. Reson. Spectrosc.* **31**, 293–315 (1997).
- R. A. Green, R. W. Adams, S. B. Duckett, R. E. Mewis, D. C. Williamson, G. G. R. Green, The theory and practice of hyperpolarization in magnetic resonance using parahydrogen. *Prog. Nucl. Magn. Reson. Spectrosc.* **67**, 1–48 (2012).
- R. W. Adams, J. A. Aguilar, K. D. Atkinson, M. J. Cowley, P. I. P. Elliott, S. B. Duckett, G. G. R. Green, I. G. Khazal, J. López-Serrano, D. C. Williamson, Reversible interactions with para-hydrogen enhance NMR sensitivity by polarization transfer. *Science* **323**, 1708–1711 (2009).
- R. W. Adams, S. B. Duckett, R. A. Green, D. C. Williamson, G. G. R. Green, A theoretical basis for spontaneous polarization transfer in non-hydrogenative parahydrogen-induced polarization. *J. Chem. Phys.* **131**, 194505 (2009).
- A. N. Pravdivtsev, A. V. Yurkovskaya, H. M. Vieth, K. L. Ivanov, R. Kaptein, Level anti-crossings are a key factor for understanding para-hydrogen-induced hyperpolarization in SABRE experiments. *ChemPhysChem* **14**, 3327–3331 (2013).
- A. N. Pravdivtsev, A. V. Yurkovskaya, K. L. Ivanov, H.-M. Vieth, Importance of polarization transfer in reaction products for interpreting and analyzing CIDNP at low magnetic fields. *J. Magn. Reson.* **254**, 35–47 (2015).
- N. Eshuis, R. L. E. G. Aspers, B. J. A. van Weerdenburg, M. C. Feiters, F. P. J. T. Rutjes, S. S. Wijmenga, M. Tessari, Determination of long-range scalar  $^1\text{H}$ - $^1\text{H}$  coupling constants responsible for polarization transfer in SABRE. *J. Magn. Reson.* **265**, 59–66 (2016).
- K. D. Atkinson, M. J. Cowley, P. I. P. Elliott, S. B. Duckett, G. G. R. Green, J. López-Serrano, A. C. Whitwood, Spontaneous transfer of parahydrogen derived spin order to pyridine at low magnetic field. *J. Am. Chem. Soc.* **131**, 13362–13368 (2009).
- P. J. Rayner, M. J. Burns, A. M. Olaru, P. Norcott, M. Fekete, G. G. R. Green, L. A. R. Highton, R. E. Mewis, S. B. Duckett, Delivering strong  $^1\text{H}$  nuclear hyperpolarization levels and long magnetic lifetimes through signal amplification by reversible exchange. *Proc. Natl. Acad. Sci. U.S.A.* **114**, E3188–E3194 (2017).
- H. Zeng, J. Xu, J. Gillen, M. T. McMahon, D. Artemov, J.-M. Tyburn, J. A. B. Lohman, R. E. Mewis, K. D. Atkinson, G. G. R. Green, S. B. Duckett, P. C. M. van Zijl, Optimization of SABRE for polarization of the tuberculosis drugs pyrazinamide and isoniazid. *J. Magn. Reson.* **237**, 73–78 (2013).
- E. B. Ducker, L. T. Kuhn, K. Münnemann, C. Griesinger, Similarity of SABRE field dependence in chemically different substrates. *J. Magn. Reson.* **214**, 159–165 (2012).
- R. E. Mewis, R. A. Green, M. C. R. Cockett, M. J. Cowley, S. B. Duckett, G. G. R. Green, R. O. John, P. J. Rayner, D. C. Williamson, Strategies for the hyperpolarization of acetonitrile and related ligands by SABRE. *J. Phys. Chem. B* **119**, 1416–1424 (2015).
- D. A. Barskiy, R. V. Shchepin, A. M. Coffey, T. Theis, W. S. Warren, B. M. Goodson, E. Y. Chekmenev, Over 20%  $^{15}\text{N}$  hyperpolarization in under one minute for metronidazole, an antibiotic and hypoxia probe. *J. Am. Chem. Soc.* **138**, 8080–8083 (2016).
- R. E. Mewis, K. D. Atkinson, M. J. Cowley, S. B. Duckett, G. G. R. Green, R. A. Green, L. A. R. Highton, D. Kilgour, L. S. Lloyd, J. A. B. Lohman, D. C. Williamson, Probing signal amplification by reversible exchange using an NMR flow system. *Magn. Reson. Chem.* **52**, 358–369 (2014).
- J. F. P. Colell, A. W. J. Logan, Z. Zhou, R. V. Shchepin, D. A. Barskiy, G. X. Ortiz Jr., Q. Wang, S. J. Malcolmson, E. Y. Chekmenev, W. S. Warren, T. Theis, Generalizing, extending, and maximizing nitrogen-15 hyperpolarization induced by parahydrogen in reversible exchange. *J. Phys. Chem. C* **121**, 6626–6634 (2017).
- D. A. Barskiy, R. V. Shchepin, C. P. N. Tanner, J. F. P. Colell, B. M. Goodson, T. Theis, W. S. Warren, E. Y. Chekmenev, The absence of quadrupolar nuclei facilitates efficient  $^{13}\text{C}$  hyperpolarization via reversible exchange with parahydrogen. *ChemPhysChem* **18**, 1493–1498 (2017).
- V. V. Zhivonitko, I. V. Skovpin, I. V. Koptuyug, Strong  $^{31}\text{P}$  nuclear spin hyperpolarization produced via reversible chemical interaction with parahydrogen. *Chem. Commun.* **51**, 2506–2509 (2015).
- M. J. Burns, P. J. Rayner, G. G. R. Green, L. A. R. Highton, R. E. Mewis, S. B. Duckett, Improving the hyperpolarization of  $^{31}\text{P}$  nuclei by synthetic design. *J. Phys. Chem. B* **119**, 5020–5027 (2015).
- B. J. A. van Weerdenburg, S. Glöggler, N. Eshuis, A. H. J. T. Engwerda, J. M. M. Smits, R. de Gelder, S. Appelt, S. S. Wijmenga, M. Tessari, M. C. Feiters, B. Blümich, F. P. J. T. Rutjes, Ligand effects of NHC-iridium catalysts for signal amplification by reversible exchange (SABRE). *Chem. Commun.* **49**, 7388–7390 (2013).
- L. S. Lloyd, A. Asghar, M. J. Burns, A. Charlton, S. Coombes, M. J. Cowley, G. J. Dear, S. B. Duckett, G. R. Genov, G. G. R. Green, L. A. R. Highton, A. J. J. Hooper, M. Khan, I. G. Khazal, R. J. Lewis, R. E. Mewis, A. D. Roberts, A. J. Ruddlesden, Hyperpolarisation through reversible interactions with parahydrogen. *Cat. Sci. Technol.* **4**, 3544–3554 (2014).
- S. Lehmkuhl, M. Emondts, L. Schubert, P. Spanning, J. Klankermayer, B. Blümich, P. P. M. Schleker, Hyperpolarizing water with parahydrogen. *ChemPhysChem* **18**, 2426–2429 (2017).
- K. X. Moreno, K. Nasr, M. Milne, A. D. Sherry, W. J. Goux, Nuclear spin hyperpolarization of the solvent using signal amplification by reversible exchange (SABRE). *J. Magn. Reson.* **257**, 15–23 (2015).
- M. Fekete, P. J. Rayner, G. G. R. Green, S. B. Duckett, Harnessing polarisation transfer to indazole and imidazole through signal amplification by reversible exchange to improve their NMR detectability. *Magn. Reson. Chem.* **55**, 944–957 (2017).
- M. L. Truong, T. Theis, A. M. Coffey, R. V. Shchepin, K. W. Waddell, F. Shi, B. M. Goodson, W. S. Warren, E. Y. Chekmenev,  $^{15}\text{N}$  hyperpolarization by reversible exchange using SABRE-SHEATH. *J. Phys. Chem. C* **119**, 8786–8797 (2015).
- H. K. Hall Jr., Correlation of the base strengths of amines<sup>1</sup>. *J. Am. Chem. Soc.* **79**, 5441–5444 (1957).
- O. Beckonert, H. C. Keun, T. M. D. Ebbels, J. G. Bundy, E. Holmes, J. C. Lindon, J. K. Nicholson, Metabolic profiling, metabolomic and metabolomic procedures for NMR spectroscopy of urine, plasma, serum and tissue extracts. *Nat. Protoc.* **2**, 2692–2703 (2007).
- T. Theis, M. Truong, A. M. Coffey, E. Y. Chekmenev, W. S. Warren, LIGHT-SABRE enables efficient in-magnet catalytic hyperpolarization. *J. Magn. Reson.* **248**, 23–26 (2014).
- S. Månsson, E. Johansson, P. Magnusson, C.-M. Chai, G. Hansson, J. S. Petersson, F. Ståhlberg, K. Golman,  $^{13}\text{C}$  imaging—A new diagnostic platform. *Eur. Radiol.* **16**, 57–67 (2006).
- J. Kurhanewicz, D. B. Vigneron, K. Brindle, E. Y. Chekmenev, A. Comment, C. H. Cunningham, R. J. DeBerardinis, G. G. Green, M. O. Leach, S. S. Rajan, R. R. Rizi, B. D. Ross, W. S. Warren, C. R. Malloy, Analysis of cancer metabolism by imaging hyperpolarized nuclei: Prospects for translation to clinical research. *Neoplasia* **13**, 81–97 (2011).
- J.-B. Hövener, N. Schwaderlapp, T. Lickert, S. B. Duckett, R. E. Mewis, L. A. R. Highton, S. M. Kenny, G. G. R. Green, D. Leibfritz, J. G. Korvink, J. Hennig, D. von Elverfeldt, A hyperpolarized equilibrium for magnetic resonance. *Nat. Commun.* **4**, 2946 (2013).
- O. G. Salnikov, K. V. Kovtunov, D. A. Barskiy, A. K. Khudorozhkov, E. A. Inozemtseva, I. P. Prosvirin, V. I. Bukhtiyarov, I. V. Koptuyug, Evaluation of the mechanism of heterogeneous hydrogenation of  $\alpha,\beta$ -unsaturated carbonyl compounds via pairwise hydrogen addition. *ACS Catal.* **4**, 2022–2028 (2014).
- C. Godard, S. B. Duckett, S. Polas, R. Tooze, A. C. Whitwood, An NMR study of cobalt-catalyzed hydroformylation using para-hydrogen induced polarisation. *Dalton Trans.* 2496–2509 (2009).
- D. J. Fox, S. B. Duckett, C. Flaschenriem, W. W. Brennessel, J. Schneider, A. Gunay, R. Eisenberg, A model iridium hydroformylation system with the large bite angle ligand xantphos: Reactivity with parahydrogen and implications for hydroformylation catalysis. *Inorg. Chem.* **45**, 7197–7209 (2006).
- D. Blazina, S. B. Duckett, P. J. Dyson, J. A. B. Lohman, Direct comparison of hydrogenation catalysis by intact versus fragmented triruthenium clusters. *Angew. Chem. Int. Ed.* **40**, 3874–3877 (2001).
- S. A. Colebrooke, S. B. Duckett, J. A. B. Lohman, R. Eisenberg, Hydrogenation studies involving halobis(phosphine)-rhodium(I) dimers: Use of parahydrogen induced polarisation to detect species present at low concentration. *Chemistry* **10**, 2459–2474 (2004).
- J. S. M. Samec, J.-E. Bäckvall, P. G. Andersson, P. Brandt, Mechanistic aspects of transition metal-catalyzed hydrogen transfer reactions. *Chem. Soc. Rev.* **35**, 237–248 (2006).
- M. Patel, R. K. Saunthwal, A. K. Verma, Base-mediated hydroamination of alkynes. *Acc. Chem. Res.* **50**, 240–254 (2017).
- J. S. Anderson, J. Rittle, J. C. Peters, Catalytic conversion of nitrogen to ammonia by an iron model complex. *Nature* **501**, 84–87 (2013).

**Acknowledgments:** We thank A. J. Holmes, M. Fekete, and A. Ruddlesden for their help. **Funding:** We thank the Wellcome Trust (092506 and 098335), the Engineering and Physical Sciences Research Council (EP/R51181X/1), and the University of York for supporting this work. **Author contributions:** W.I., P.J.R., and S.B.D. all contributed equally to the preparation of this manuscript. W.I. and P.J.R. collected the raw data, and all authors were involved in the interpretation of results

and design of experiments. **Competing interests:** W.I., P.J.R., and S.B.D. are inventors on a patent application filed by the University of York based on this work (patent no. GB 1711967.8, filed 25 July 2017). The authors declare that they have no other competing interests. **Data and materials availability:** All data needed to evaluate the conclusions in the paper are present in the paper and/or the Supplementary Materials. All relevant plasmids and experimental data may be requested from the authors. Raw data can be found via DOI: 10.15124/d93f83bf-9fc7-4cf8-8267-504a0304a516.

Submitted 9 August 2017  
Accepted 29 November 2017  
Published 5 January 2018  
10.1126/sciadv.aao6250

**Citation:** W. Iali, P. J. Rayner, S. B. Duckett, Using *parahydrogen* to hyperpolarize amines, amides, carboxylic acids, alcohols, phosphates, and carbonates. *Sci. Adv.* **4**, eaao6250 (2018).

## Using *parahydrogen* to hyperpolarize amines, amides, carboxylic acids, alcohols, phosphates, and carbonates

Wissam Iali, Peter J. Rayner and Simon B. Duckett

*Sci Adv* 4 (1), eaao6250.  
DOI: 10.1126/sciadv.aao6250

### ARTICLE TOOLS

<http://advances.sciencemag.org/content/4/1/eaao6250>

### SUPPLEMENTARY MATERIALS

<http://advances.sciencemag.org/content/suppl/2017/12/22/4.1.eaao6250.DC1>

### REFERENCES

This article cites 39 articles, 2 of which you can access for free  
<http://advances.sciencemag.org/content/4/1/eaao6250#BIBL>

### PERMISSIONS

<http://www.sciencemag.org/help/reprints-and-permissions>

Use of this article is subject to the [Terms of Service](#)

---

*Science Advances* (ISSN 2375-2548) is published by the American Association for the Advancement of Science, 1200 New York Avenue NW, Washington, DC 20005. 2017 © The Authors, some rights reserved; exclusive licensee American Association for the Advancement of Science. No claim to original U.S. Government Works. The title *Science Advances* is a registered trademark of AAAS.